SUPPLEMENTARY INFORMATION

An octahedral coordination cage with six Fe(III) centers as a T_1 MRI probe

Aruni Dissanayake,[a] Joseph A. Spernyak,[b] and Janet R. Morrow[a]*

[a] Department of Chemistry, University at Buffalo, State University of New York, Amherst, New York 14260, United States
[b] Department of Cell Stress Biology, Roswell Park Comprehensive Cancer Center, New York 14263, United States

Contents

01. Instrumentation and materials

Instrumentation

A Bruker Neo 500 NMR spectrometer (broadband, autosampler) operating at 500 MHz, or 126 MHz was used to collect ^{1}H NMR spectra or ^{13}C NMR spectrum, respectively. The same instrument operating at 500 MHz was used to acquire the 2D-COSY NMR spectrum and the DOSY NMR spectrum. Chemical shifts (δ) were reported in parts per million (ppm) and corrected to residual proteo-solvent peaks. ^{17}O NMR spectra were acquired using a Varian Inova 9.4 T spectrometer with a 5 mm broad-band probe operating at 54.24 MHz. pH measurements were obtained using a Thermo Scientific 9110DJWP double junction, glass, semi-micro pH electrode connected to a 702 SM Titrino pH meter. A Thermo Fisher Linear Ion Trap (LTQ) Mass Spectrometer was used to collect all mass spectral data. High-resolution mass spectrometry data was collected using a Thermo Scientific Q-Exactive Focus Orbitrap® Tandem Mass Spectrometer with UltiMate 3000 liquid chromatography. Absorbance spectra were collected using a Beckman-Coulter DU 800 UV–Vis Spectrophotometer equipped with a Peltier temperature controller. Cyclic voltammograms were collected using a WavenowXV potentiostat from Pine Research using a glassy carbon working electrode, an Ag/AgCl reference electrode, and a Pt counter electrode, all purchased from Pine Research. Iron concentration of the cage was determined by using a Thermo X-Series 2 inductively coupled plasma mass spectrometer (ICP-MS). T_1 and T_2 relaxation time values were obtained using a Nanalysis (1.4 T) NMReady-60 Benchtop 60 MHz spectrometer. In vivo, MR imaging was performed at 7 T per approved Roswell Park IACUC protocols.

Materials

Solvents and reagents were used without further purification unless otherwise specified. Trimethyl-1,3,5- benzene-tricarboxylate was purchased from TCI America. Salicylaldehyde, hydrazine monohydrate (98%), human serum albumin (HSA), apo-transferrin, warfarin, iodipamide, methyl orange, 8-hydroxypyrene-1,3,6-trisulfonic acid trisodium salt (HPTS) and poly-L-lysine were purchased from Sigma Aldrich. Gallium(III) acetylacetonate ($Ga(acac)_3$) and Iron(III) acetylacetonate ($Fe(acac)_3$) were purchased from BeanTown Chemical. Ibuprofen was purchased from Alfa Aesar. 65–70% nitric acid with greater than 99.999% purity (trace metals basis) was purchased from BeanTown Chemical. Benzene-1,3,5-tricarbohydrazide (2) was synthesized as reported previously[1].

02. Synthesis and characterization

2.1. Synthesis of H_6L ligand (3)

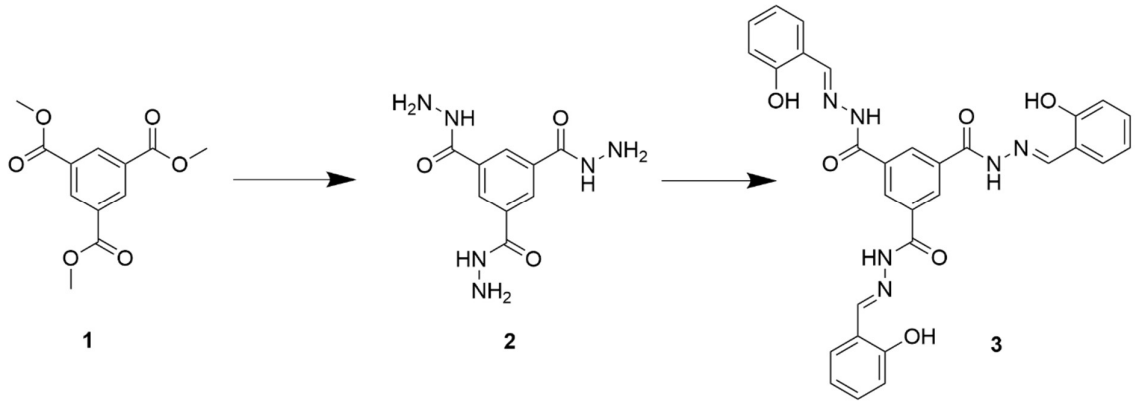

Scheme S1. Synthetic route of ligand H_6L

The preparation of the H_6L ligand was adopted from the literature[2]. Salicylaldehyde (0.82 g, 6.5 mmol) was added to a methanolic solution (50 mL) of benzene-1,3,5-tricarbohydrazide **(2)** (0.50 g, 2.0 mmol). After adding 5 drops of glacial acetic acid, the mixture was heated at reflux for 12 hours. The white precipitate formed during the reaction was collected by vacuum filtration, washed with methanol, and dried under vacuum. 1.0 g (92%) of product **3** was collected. ESI-MS in 60: 40 methanol: water *m/z* = $[M + Na]^+$ calculated for $C_{30}H_{24}N_6O_6Na$, 587.17; found 587.25 (M= H_6L). ^1H NMR (500 MHz, DMSO-d_6) δ 12.44 (s, 3H), 11.17 (s, 3H), 8.74 (d, J = 4.6 Hz, 6H), 7.63 (dd, J = 7.7, 1.7 Hz, 3H), 7.37 – 7.30 (m, 3H), 6.99 – 6.92 (m, 6H) ppm. ^{13}C NMR (126 MHz, DMSO-d_6) δ 161.6, 157.5, 148.7, 133.8, 131.7, 130.1, 129.3, 119.5, 118.8, 116.5 ppm.

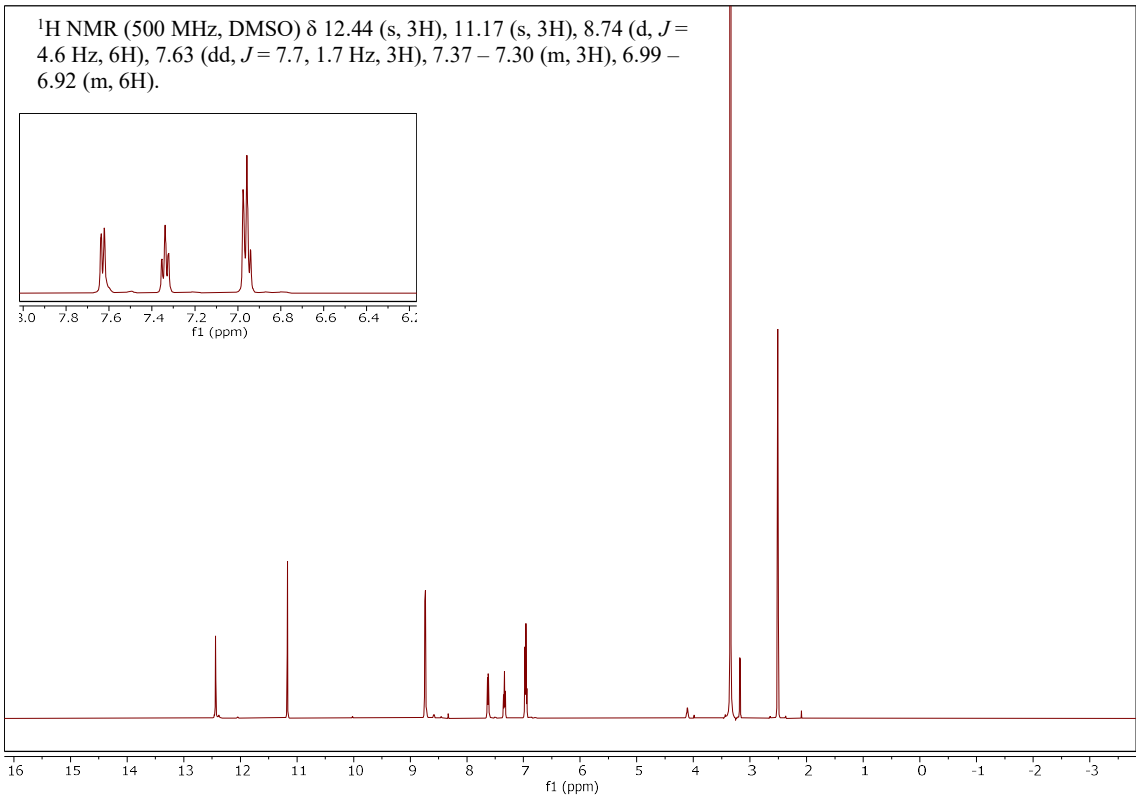

Figure S1. ^{1}H NMR (500 MHz, DMSO-d_6) of H_6L

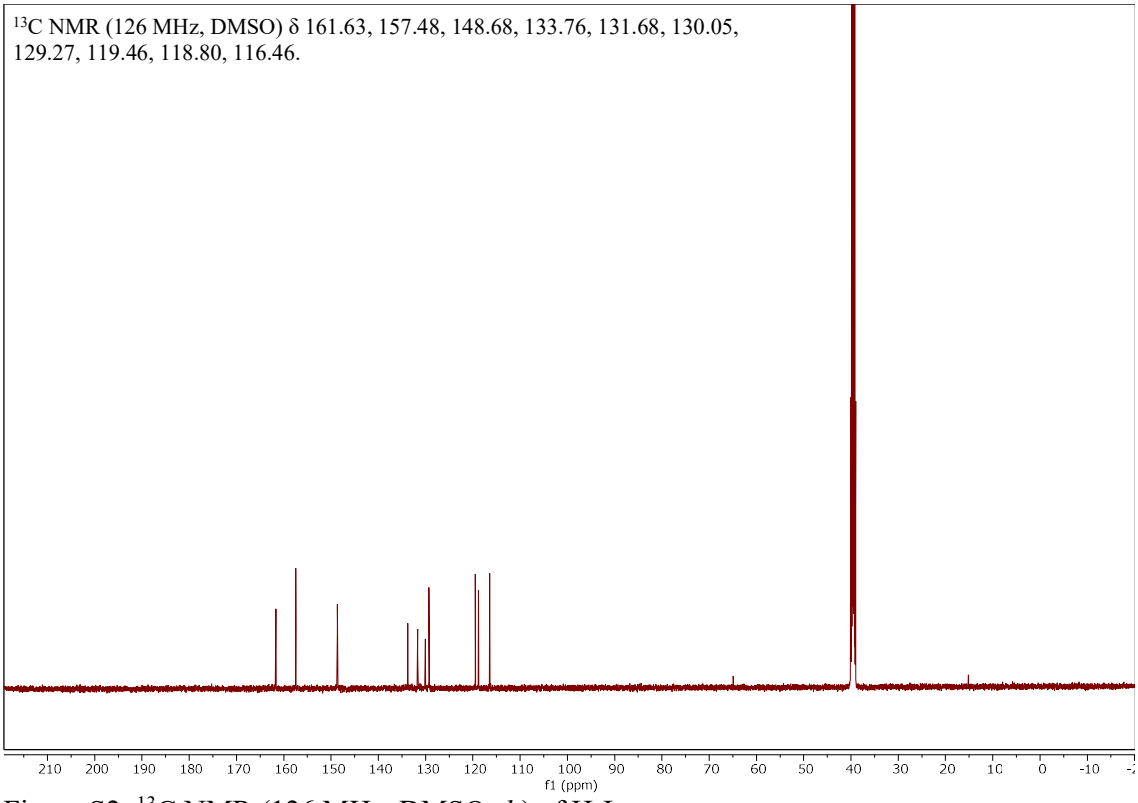

Figure S2. ^{13}C NMR (126 MHz, DMSO-d_6) of H_6L

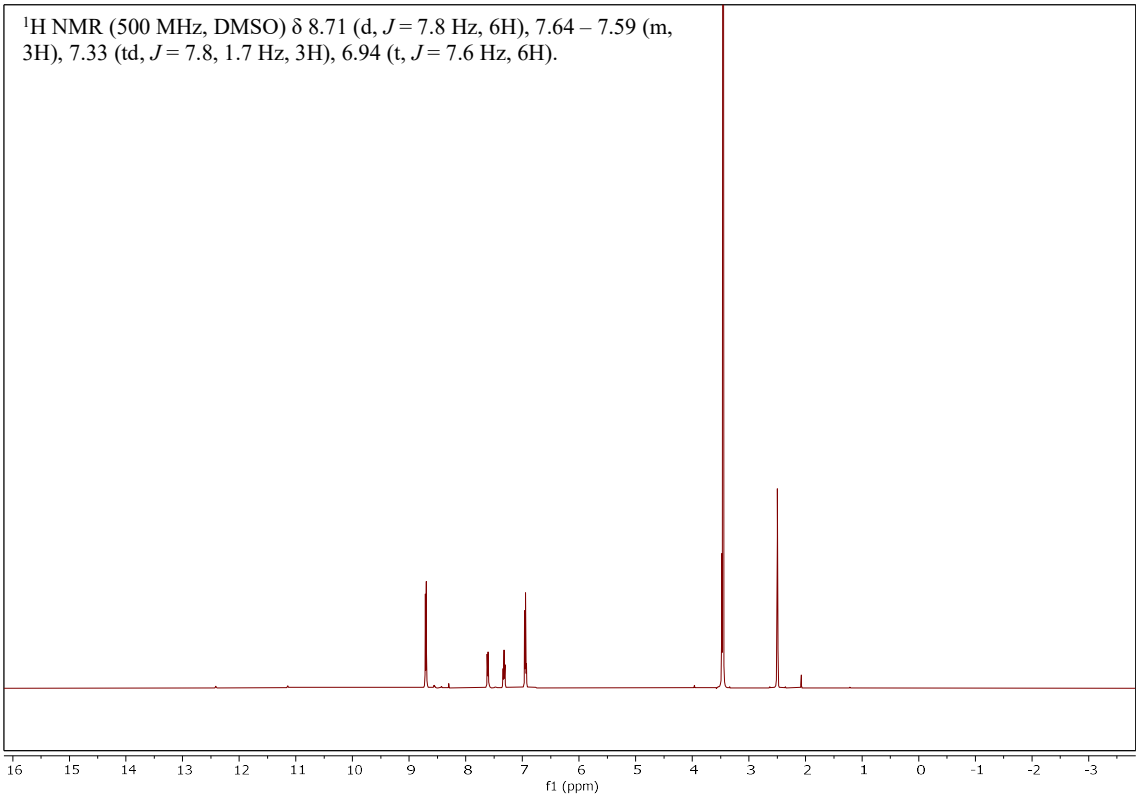

Figure S3. [1]H NMR (500 MHz, DMSO-d_6) of H_6L in the presence of a drop of D_2O.

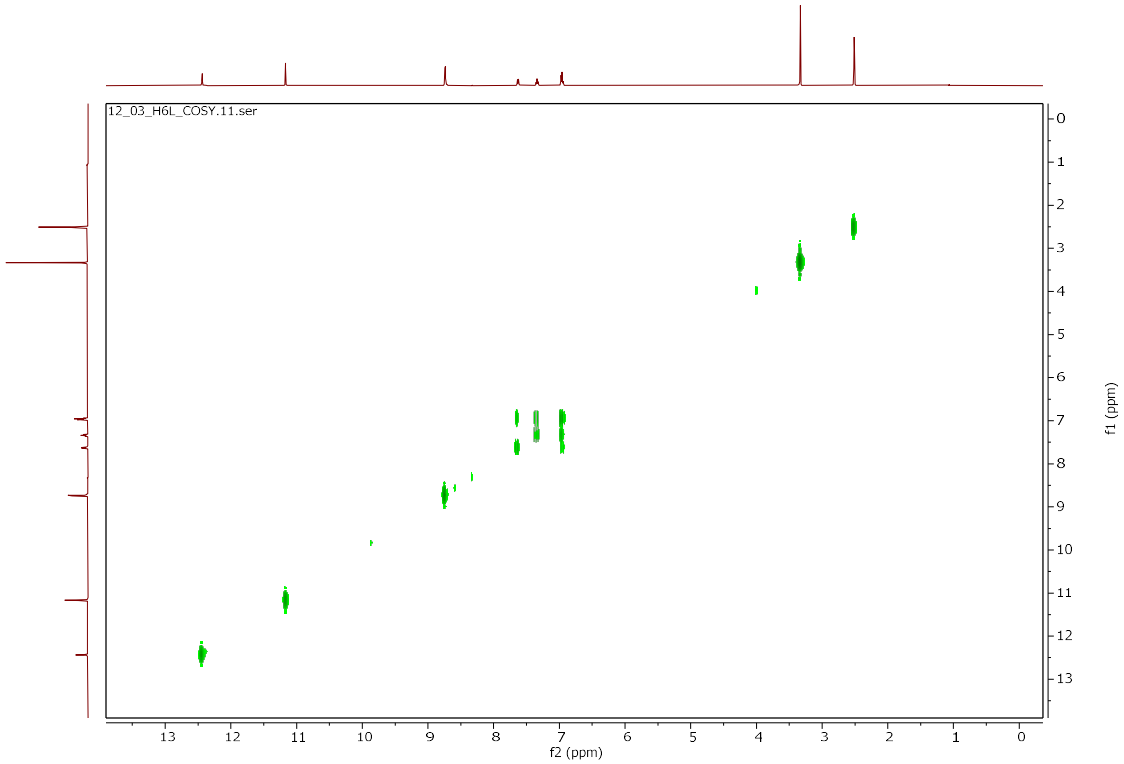

Figure S4. [1]H-COSY NMR (500 MHz, DMSO-d_6) of H_6L

2.2. Synthesis of $K_6[Ga_6L_4]$

Synthesis of $K_6[Ga_6L_4]$ was adapted from a previous literature procedure[3]. Ligand H_6L (0.100 g, 0.177 mmol) was added to 6 mL of dry methanol under an inert atmosphere. $Ga(acac)_3$ (97.6 mg, 0.266 mmol) was added to the solution which turned the solution into pale-yellow. Potassium hydroxide (14.9 mg, 0.266 mmol) dissolved in dry methanol was added to the mixture which rapidly turned into bright yellow. The solution was stirred overnight under argon. About 25 mL of diethyl ether was added to the clear solution dropwise and a pale-yellow solid product was isolated. (40% yield). ^{1}H NMR (500 MHz, DMSO- d_6) δ 8.78 (s, 12H), 8.37 (s, 12H), 7.35 (d, J = 7.8 Hz, 12H), 7.19 (t, J = 7.9 Hz, 12H), 6.63 (t, J = 7.5 Hz, 12H), 6.53 (d, J = 8.4 Hz, 12H) ppm. Purity was determined as 94% by ^{1}H NMR integration against methyl-3,5- dinitrobenzoate standard.

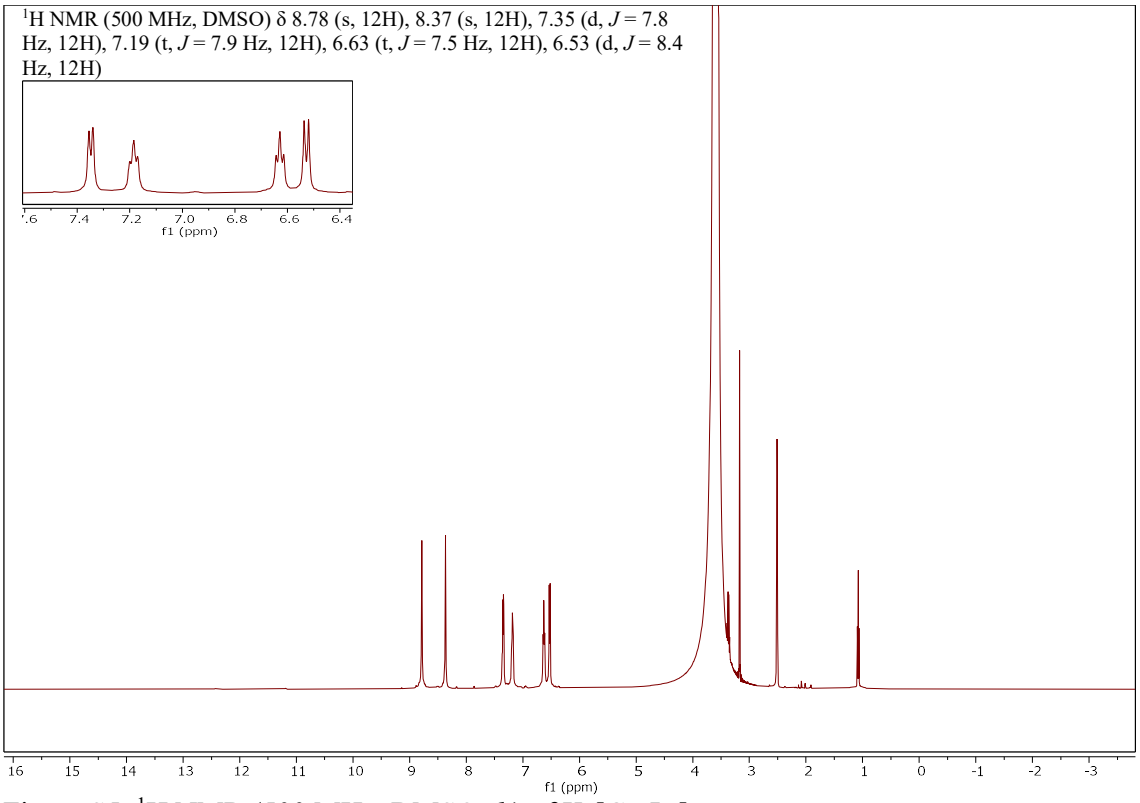

Figure S5. ^{1}H NMR (500 MHz, DMSO-d_6) of $K_6[Ga_6L_4]$

2.3. Stokes-Einstein determination of the solute radius of Ga_6L_4 cage

The Stokes-Einstein equation (Equation 1) was used to estimate the hydrodynamic diameter of the analogous Ga_6L_4 cage.

$$D = \frac{k_B T}{6\pi\mu R_0} \qquad \text{Equation S1}$$

The self-diffusion constant (D) of the Ga_6L_4 cage was determined by the gradient-compensated stimulated echo DOSY experiment, which was used to estimate the molecular size according to the above equation, where k_B is the Boltzmann constant (1.38×10^{-23} JK $^{-1}$), T is the

temperature given in Kelvin, μ is the viscosity of the solution (1.99×10^{-3} Pa.s for DMSO at 298 K), and R_0 is the van der Waals radius of the molecule in meters.

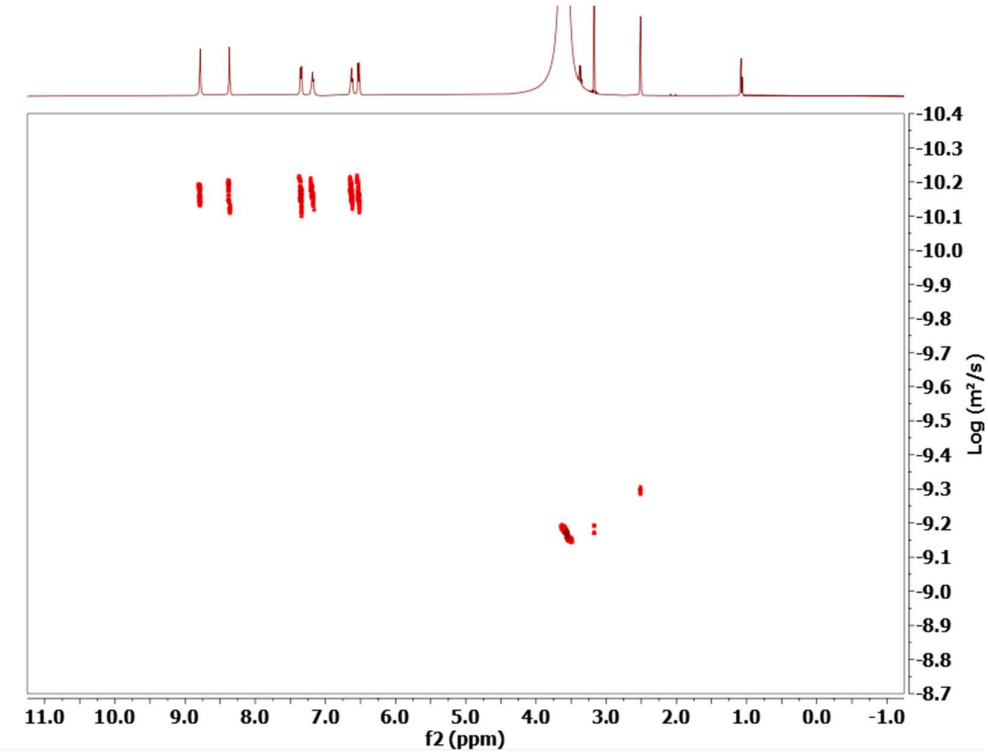

Figure S6. ^{1}H DOSY NMR (500 MHz, DMSO-d_6) spectrum of $K_6[Ga_6L_4]$. The self-diffusion constant (D) in DMSO was 7.1 x 10^{-11} m^2/s.

2.4. ESI- HRMS of Ga_6L_4 cage

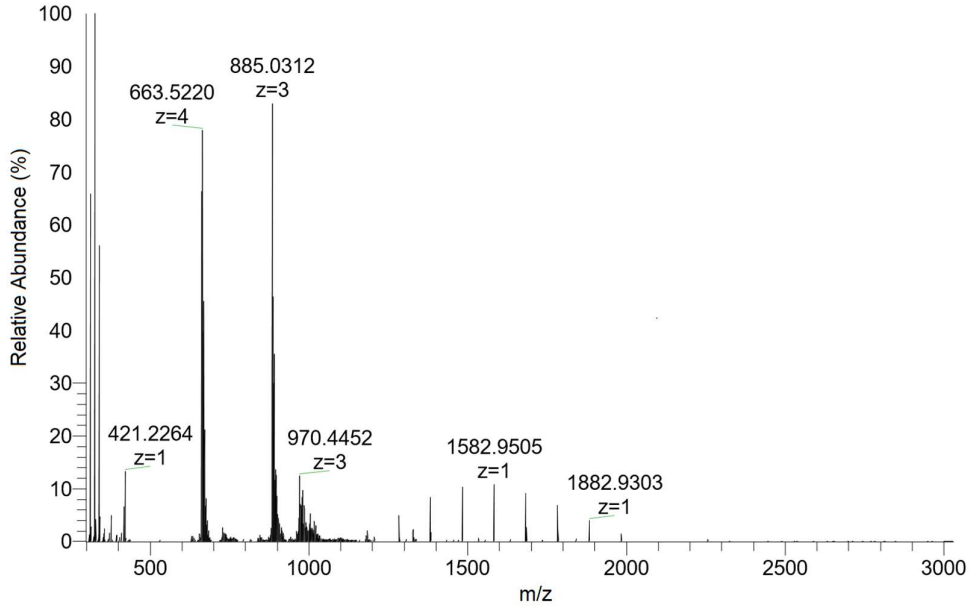

Figure S7. ESI-HRMS ((-) mode) of Ga_6L_4 in acetonitrile

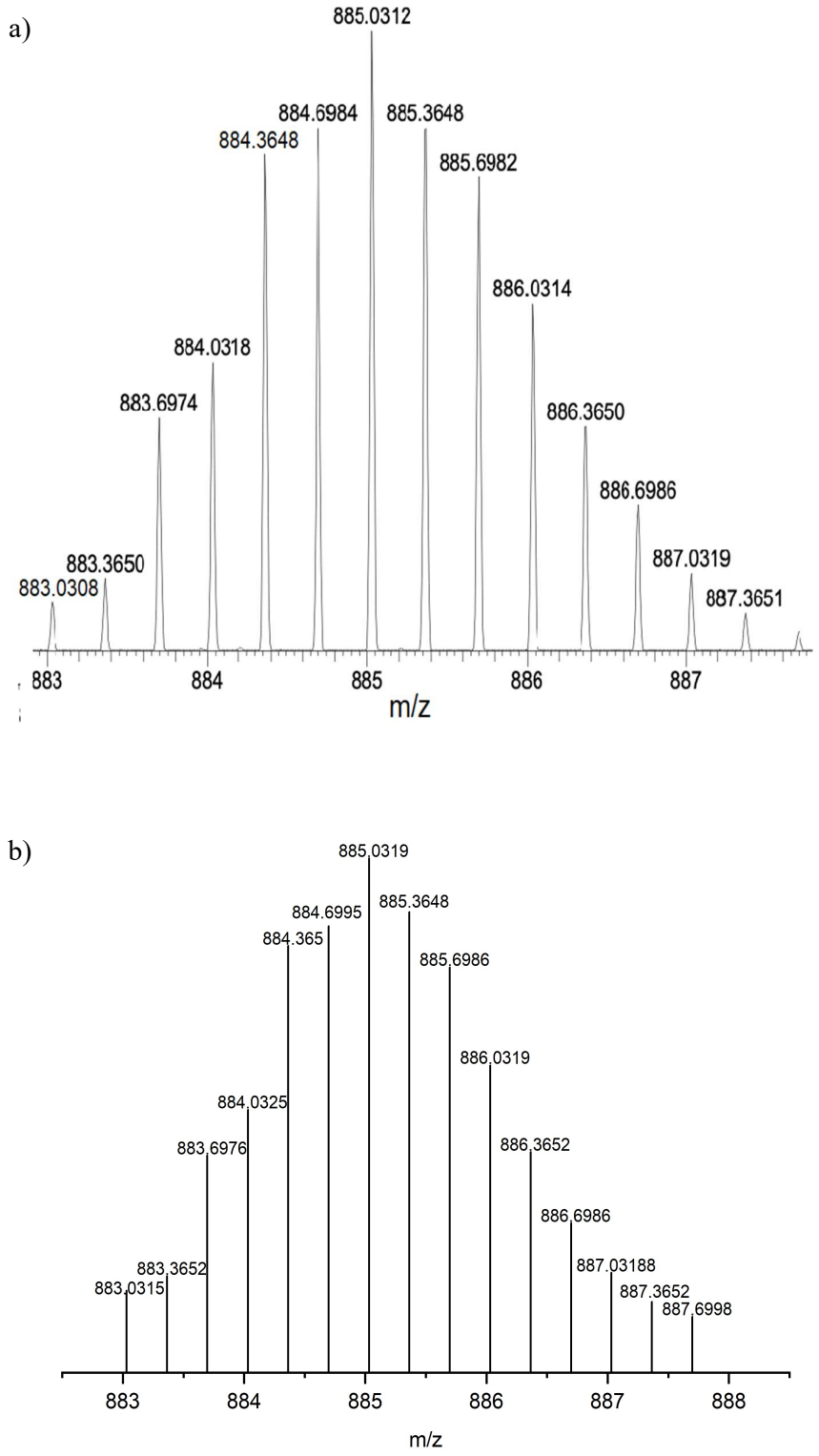

Figure S8. ESI- HRMS of $[Ga_6L_4 + 3H^+]^{3-}$ peak with the a) observed isotope distribution pattern and b) theoretical isotope distribution pattern

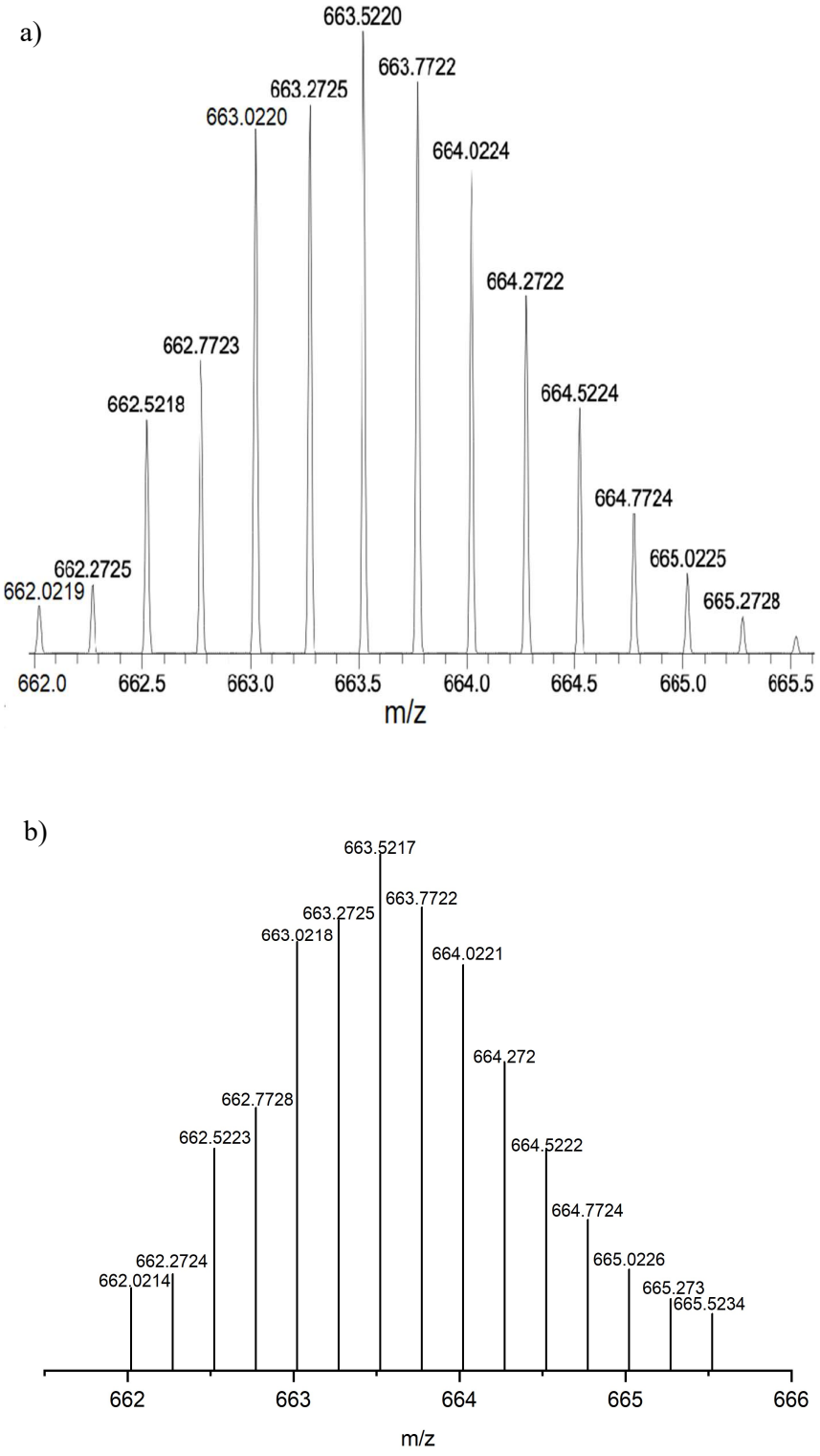

Figure S9. ESI- HRMS of $[Ga_6L_4 + 2H^+]^{4-}$ peak with the a) observed isotope distribution pattern and b) theoretical isotope distribution pattern

2.5. Synthesis of $K_6[Fe_6L_4]$

$K_6[Fe_6L_4]$ was prepared by following an analogous procedure to that of the Ga(III) cage. Ligand H_6L (0.100 g, 0.177 mmol) was added to 6 mL of dry methanol under argon. Upon the addition of $Fe(acac)_3$ (93.9 mg, 0.266 mmol), the solution rapidly turned to brick red and further turned into deep red with the addition of potassium hydroxide (14.9 mg, 0.266 mmol). The solution was stirred overnight under an inert atmosphere. About 25 mL of diethyl ether was added to the clear solution dropwise and a black solid product was isolated. (60% yield).

The solutions containing 0.17 μM of $K_6[Fe_6L_4]$ (≈1 μM Fe) were digested with 70% metal-free HNO_3 acid and assessed for purity using ICP-MS determination of iron. The expected Fe concentration of the sample was 56 ppb Fe and experimentally determined as 51.5 ± 0.5 ppb or 92% of the expected Fe content.

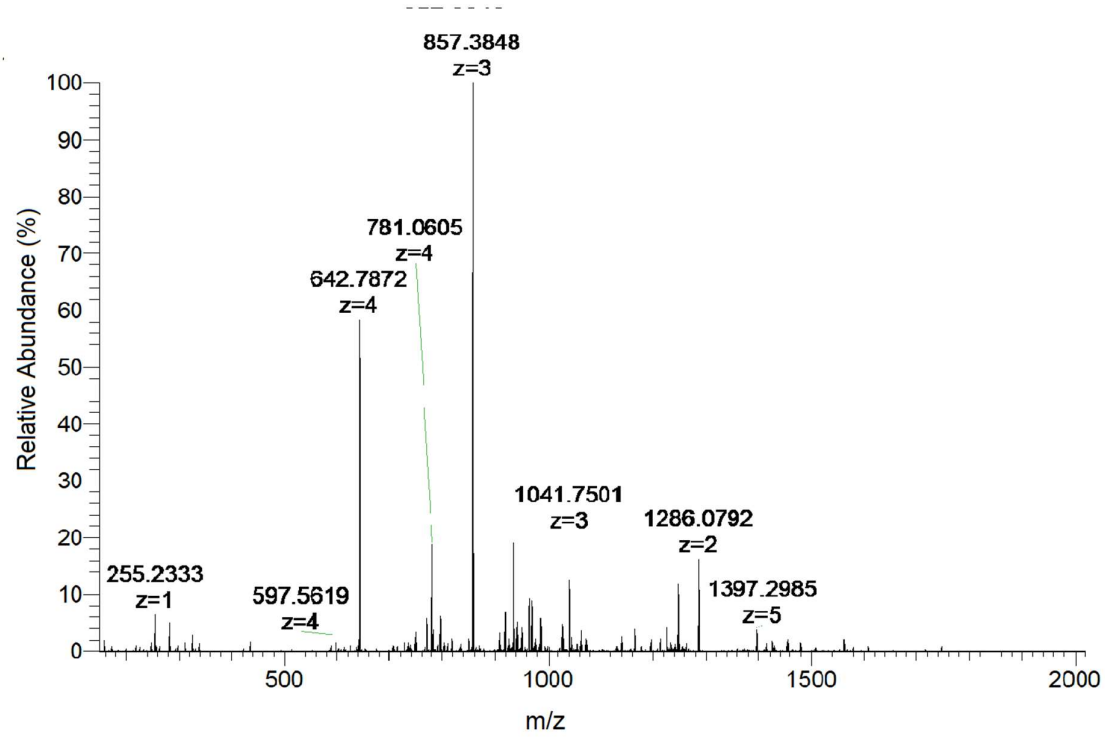

Figure S10. ESI-HRMS ((-) mode) of Fe_6L_4 in acetonitrile

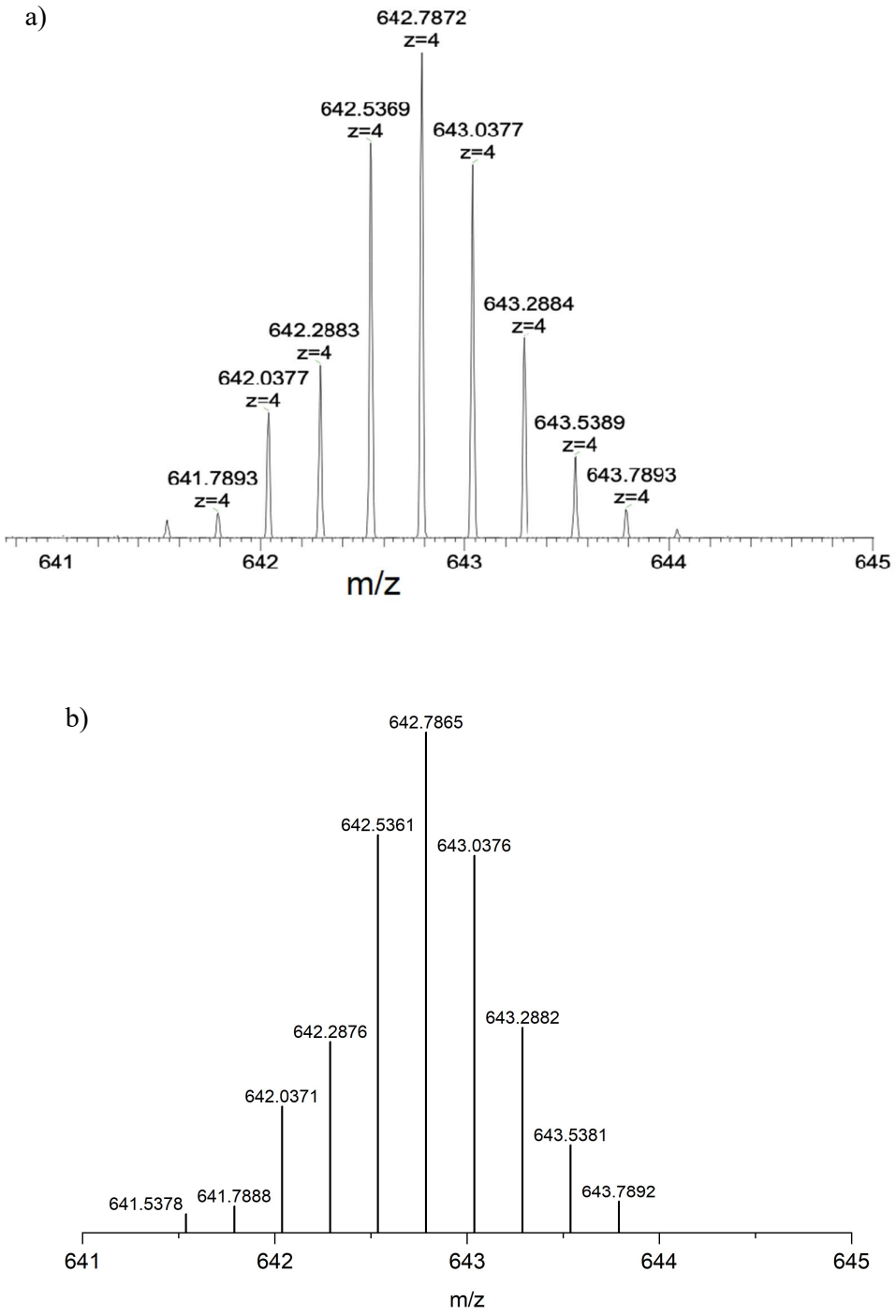

Figure S11. ESI- HRMS of $[Fe_6L_4 + 2H^+]^{4-}$ peak with the a) observed isotope distribution pattern and b) theoretical isotope distribution pattern

03. Kinetic inertness studies

The ligand-to-metal charge transfer (LMCT) band of the absorbance spectrum was used to probe the kinetic inertness of the Fe_6L_4 cage over the course of 4 hours. Temperature was controlled at 37 °C throughout the experiment by using a Peltier temperature controller. The absorbance change was monitored by both full wavelength scans between 220 nm – 820 nm and by tracking the maximum absorbance associated with the LMCT band.

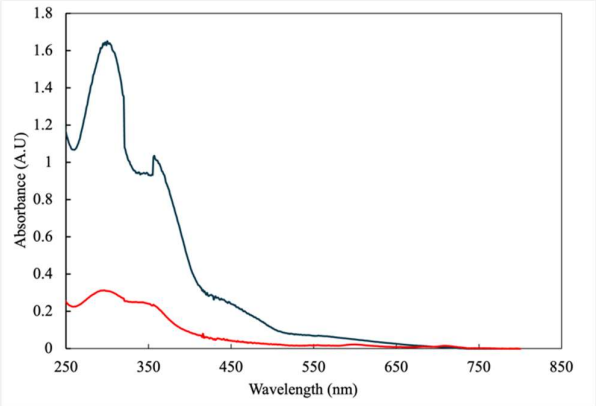

Figure S12. UV-Vis spectra of 10 µM Fe_6L_4 cage (blue) and 6 µM H_6L (red) in 1x PBS (pH 7.4)

3.1. Anions

The kinetic inertness of the Fe_6L_4 cage in the presence of biologically relevant anions was monitored on a solution containing 8 µM of the Fe_6L_4 cage in 1x PBS buffer pH adjusted to 7.4.

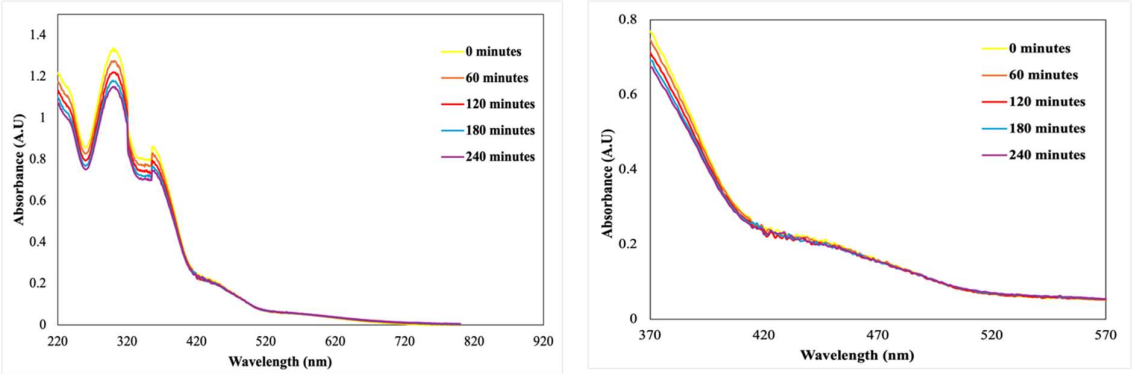

Figure S13. UV-Vis spectra of 8 µM Fe_6L_4 cage in 1x PBS (pH 7.4) at 37 °C over 4 hours (left).LMCT band of 8 µM Fe_6L_4 cage in 1x PBS (pH 7.4) at 37 °C over 4 hours (right).

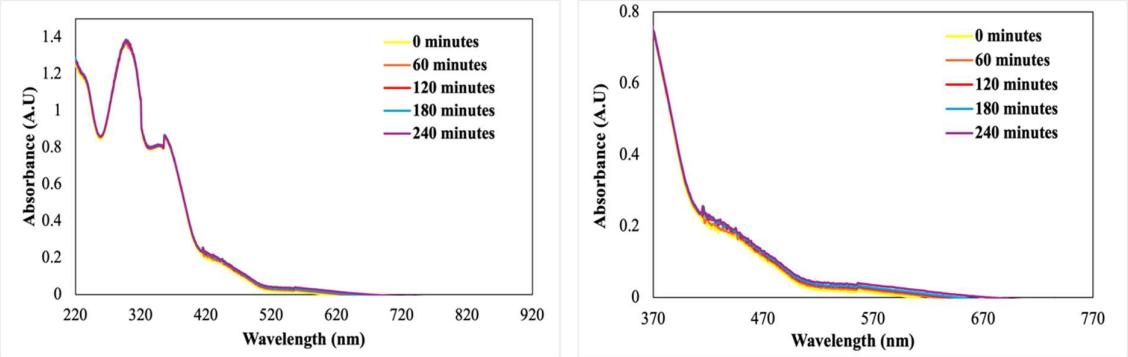

Figure S14. UV-Vis spectra of 8 μM Fe_6L_4 cage in meglumine solution (pH 7.4) at 37 °C over 4 hours (left). LMCT band of 8 μM Fe_6L_4 cage in meglumine solution (pH 7.4) at 37 °C over 4 hours (right).

3.2. Cations

Transmetallation studies were performed in the presence of excess zinc chloride (1: 10 molar ratio of Fe_6L_4 cage to $ZnCl_2$) in 1x PBS buffer pH adjusted to 7.4.

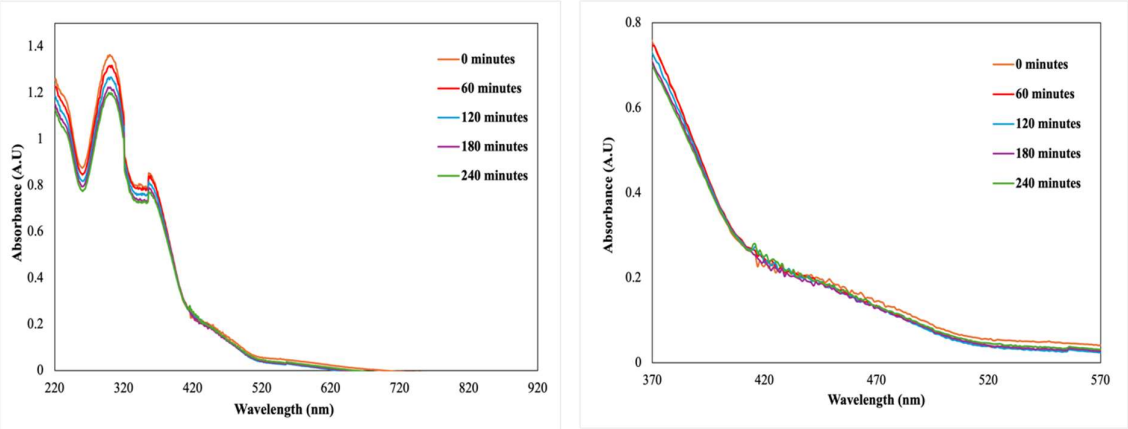

Figure S15. UV-Vis spectra of 8 μM Fe_6L_4 cage in 1x PBS (pH 7.4) at 37 °C over 4 hours with 10 equivalents of $ZnCl_2$ (left). LMCT band of 8 μM Fe_6L_4 cage in 1x PBS (pH 7.4) at 37 °C over 4 hours with 10 equivalents of $ZnCl_2$ (right).

3.3. EDTA

The stability of the Fe_6L_4 cage in the presence of excess EDTA ((1: 6 molar ratio of Fe_6L_4 cage to EDTA) was monitored in 1x PBS buffer pH adjusted to 7.4.

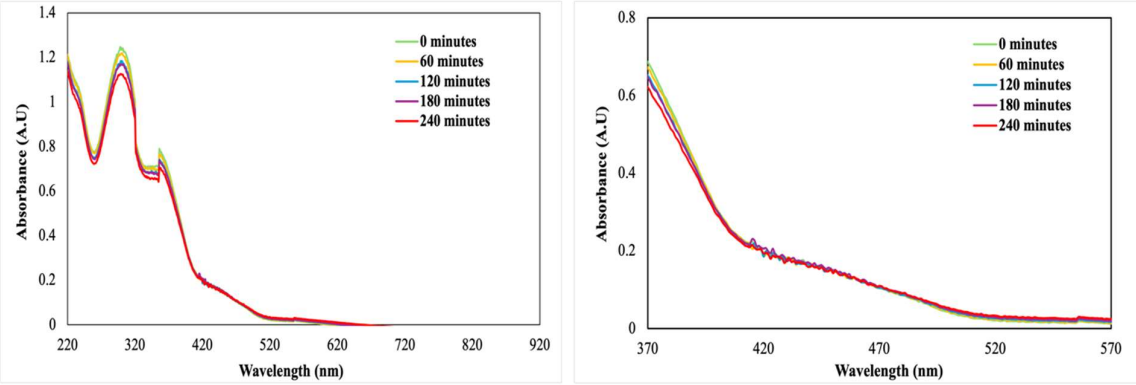

Figure S16. UV-Vis spectra of 8 μM Fe_6L_4 cage in 1x PBS (pH 7.4) at 37 °C over 4 hours with 6 equivalents of EDTA (left). LMCT band of 8 μM Fe_6L_4 cage in 1x PBS (pH 7.4) at 37 °C over 4 hours with 6 equivalents of EDTA (right).

3.4. Transferrin

The kinetic inertness of the Fe_6L_4 cage in the presence of 12 equivalents of transferrin was monitored with a solution containing 8 μM of the Fe_6L_4 cage in 1x PBS buffer pH adjusted to 7.4.

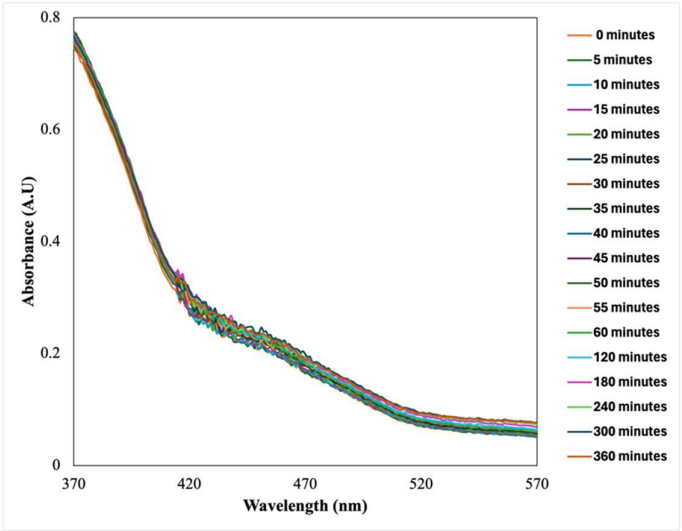

Figure S17. LMCT band of 8 μM Fe_6L_4 cage in 1x PBS (pH 7.4) at 37 °C over 6 hours with 12 equivalents of transferrin. A change in the LMCT band at 468 nm was expected[4].

04. Effective magnetic moment

The effective magnetic moment (μ_{eff}) of the $K_6[Fe_6L_4]$ cage was calculated by using the Evans method[5] at 298 K (T). A 2.00 mM sample of the $K_6[Fe_6L_4]$ cage was prepared using a solution of 5% t-butanol in D_2O (v/v) with pH adjusted to 9.0. The prepared solution was then placed in a coaxial NMR insert which was placed inside a 5 mm NMR tube containing a solution of 5% t-butanol in D_2O (v/v) as a diamagnetic standard.

$$\chi_g = \frac{3\Delta f}{4\pi f m} + \chi_0 \qquad \text{Equation S2}$$

$$\chi_m^p = \chi_m - \chi_m^{dia} \qquad \text{Equation S3}$$

$$\mu_{eff} = 2.84\,(\chi_m^p T)^{1/2} \qquad \text{Equation S4}$$

Equation 2 was used to calculate the mass susceptibility (χ_g), where Δf is the frequency shift (Hz), f is the frequency of the NMR spectrometer (Hz), m is the concentration of the paramagnetic substance (g/ mL), and χ_o is the mass susceptibility of the solvent. Mass susceptibility (χ_g) was multiplied by the molar mass of the cage to calculate the molar susceptibility (χ_m). The paramagnetic molar susceptibility (χ_m^p) was calculated by subtraction of the diamagnetic susceptibility contribution (χ_m^{dia}) as reported[6]. χ_m^p was further used to determine the magnetic moment of the $K_6[Fe_6L_4]$ cage using Equation 4.

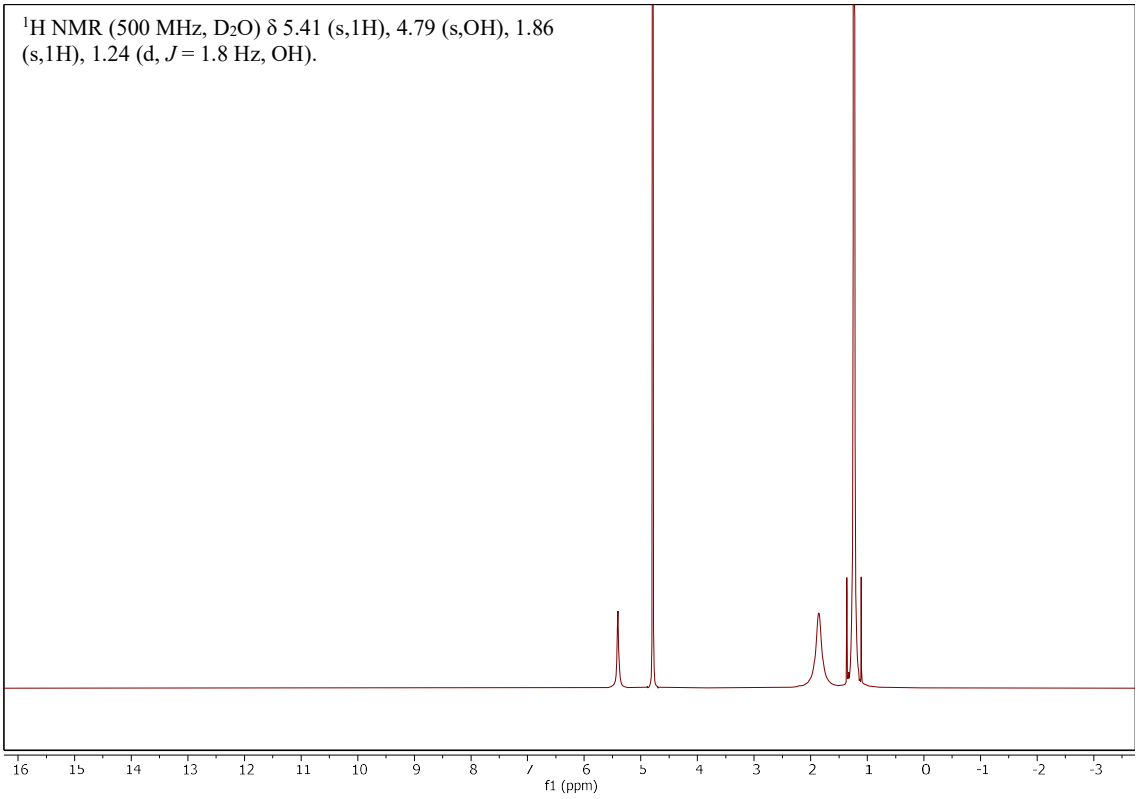

Figure S18. ^{1}H NMR (500 MHz) of 2 mM $K_6[Fe_6L_4]$ solution prepared in 5% t-butanol in D_2O (v/v)

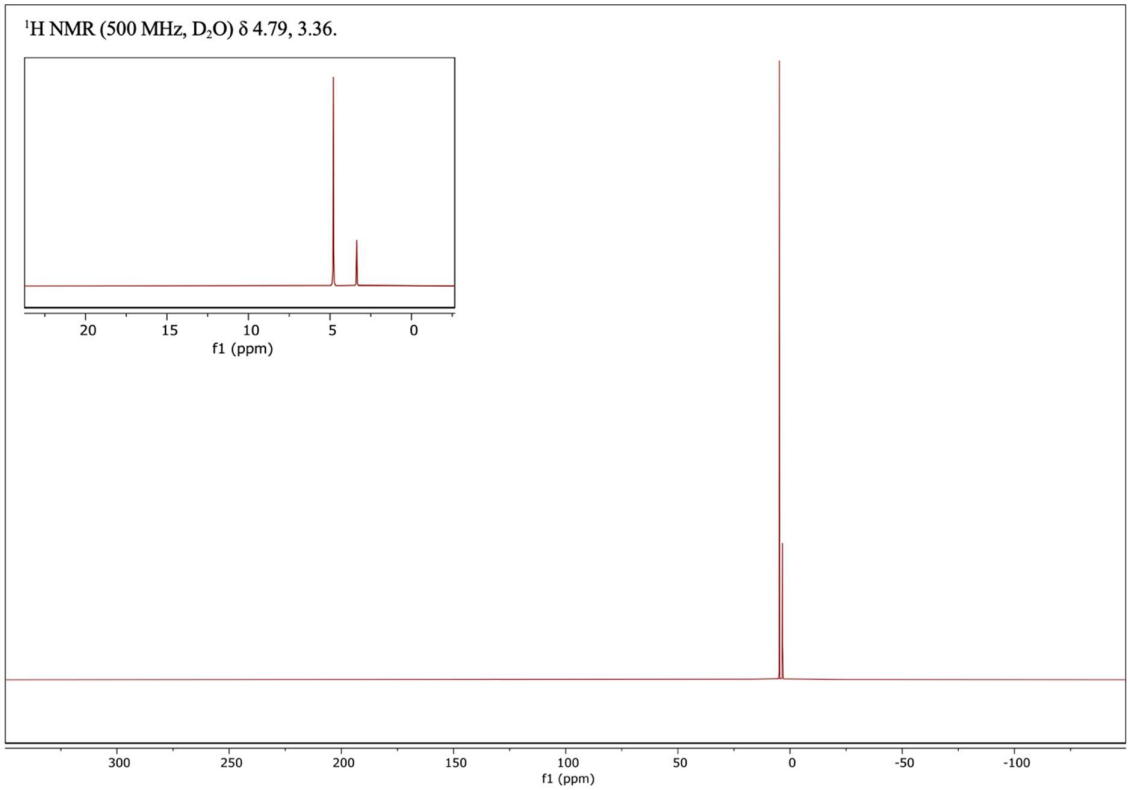

Figure S19- ^{1}H NMR (500 MHz, D_2O) of 2 mM $K_6[Fe_6L_4]$.

05. Cyclic voltammetry

The Fe(II)/Fe(III) redox potential of the Fe_6L_4 cage was studied by using cyclic voltammetry in solutions containing 0.4 mM Fe_6L_4 cage, 1 mM ferrocene in 0.1 M tetrabutylammonium hexafluorophosphate as the supporting electrolyte and acetonitrile as the solvent. The samples were purged with nitrogen for ~5 minutes before scanning. The current was measured from − 2 V to + 1 V with a 10 second pre-scan delay at variable sweep rates of 50, 100 and 200 mV/s.

The redox potential of Fe(II)/Fe(III) was calculated from the average of the anodic (E_{pa}) and the cathodic (E_{pc}) potentials with reference to Fc/Fc^+ and then converted to the normal hydrogen electrode (NHE). Redox potential of Fe(II)/Fe(III) was determined as -1.45 V vs Fc/Fc^+ or -0.83 V vs NHE.

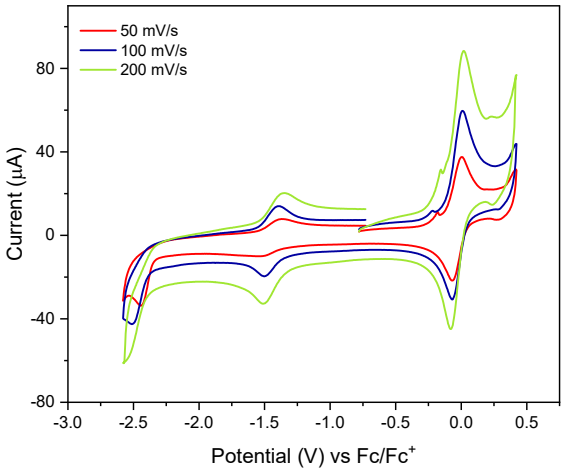

Figure S20. Cyclic voltammetry of Fe_6L_4 cage recorded with different sweep rates. Ferrocene standard is included.

06. Relaxivity studies

6.1. Proton relaxivity of Fe_6L_4

Solutions of 20, 40, 60, 80, 100 μM of the Fe_6L_4 cage were prepared in 1 x PBS solutions with a pH adjusted to 7.4 with and without 35 g/ L HSA and incubated for 30 minutes at 34 °C before measuring T_1 and T_2 relaxation times. The T_1 relaxation times of the prepared solutions were measured on a Nanalysis 1.4 T benchtop NMR at 34 °C using an inversion recovery scan. The T_2 relaxation times of the prepared solutions were measured by using multi-echo, Carr-Purcell-Meiboom-Gill spin-echo sequence. The r_1 and r_2 relaxivity values were determined by using linear regression fitting of $1/T_1$ (s^{-1}) and $1/T_2$ (s^{-1}) versus concentration (mM).

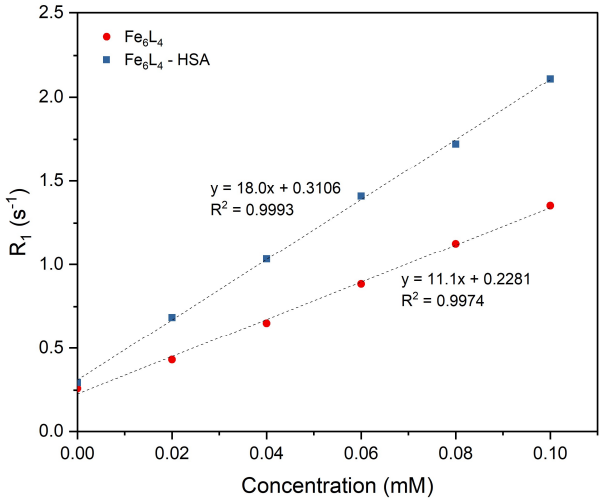

Figure S21. r_1 relaxivity determination (1.4 T, 34 °C) of Fe_6L_4 cage in 1x PBS, pH 7.4 with and without 35 mg/mL HSA.

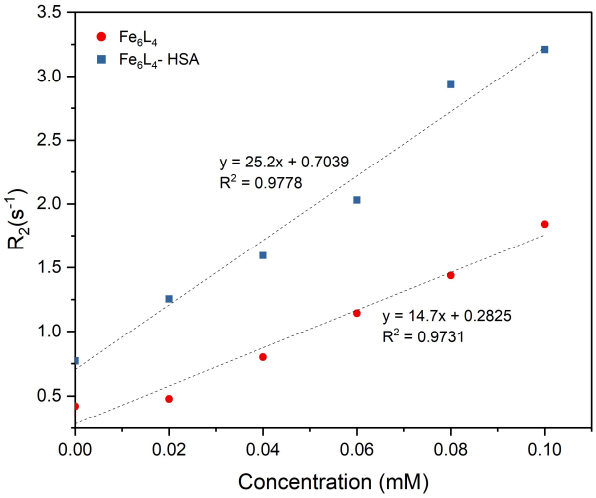

Figure S22. r_2 relaxivity determination (1.4 T, 34 °C) of Fe_6L_4 cage in 1x PBS, pH 7.4 with and without 35 mg/mL HSA.

6.2. pH dependence of r_1 relaxivity

A solution of 80.0 µM of Fe_6L_4 cage in 1 x PBS was prepared and the pH was adjusted to the desired values using NaOH or HCl solutions. Samples were incubated for 30 minutes at 34 °C before measuring T_1 relaxation times using an inversion recovery scan. Solutions of 1x PBS with pH adjusted to the desired values were used as the blank solutions.

07. ^{17}O Variable-Temperature NMR spectroscopy

The transverse relaxation rates of ^{17}O water in the samples were determined over a temperature range of 25-75 °C using the full width at half maximum (FWHM) of the ^{17}O resonance related to water in the samples. 1 mM Fe_6L_4 aqueous sample was prepared to have a final enriched concentration of 1% $^{17}OH_2$ with a pH of 7.5 (Meglumine was used to increase the solubility). The transverse relaxation rate constants ($1/T_2$) were calculated by the difference of the FWHM of the ^{17}O resonance with and without Fe_6L_4 cage and multiplying by a factor of π[7]. Transverse relaxivities (r_2^o) were calculated by normalizing $1/T_2$ values to Fe(III) concentration.

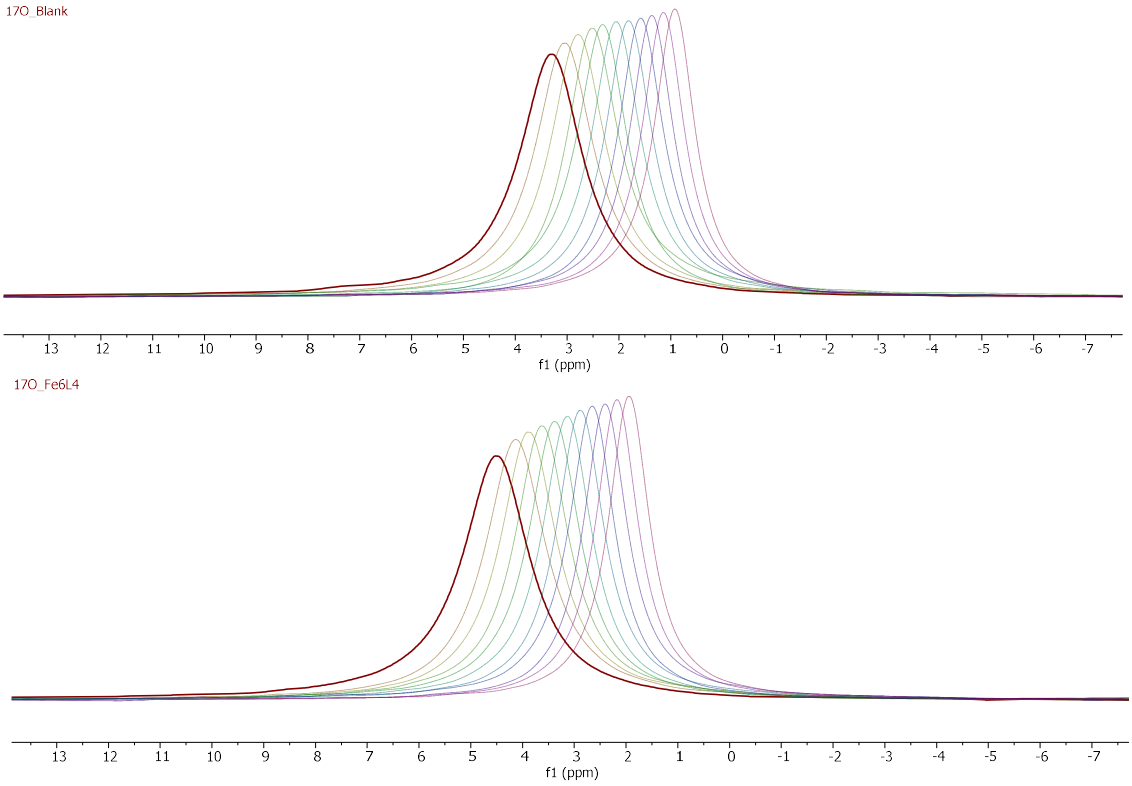

Figure S23. Variable temperature ^{17}O resonances of 1% $^{17}OH_2$ standard solution (Top) and 1 mM Fe_6L_4 sample with 1% $^{17}OH_2$ at pH of 7.5 (Bottom). NMR spectra were recorded over a temperature range of 25-75 °C, increasing left to right.

08. Protein Interactions

8.1. HSA Titration

A series of solutions were prepared, having a fixed Fe_6L_4 concentration (100 µM) in 1 x PBS (pH adjusted to 7.4) solution with an HSA concentration ranging from 0 to 100 µM. Prepared solutions were allowed to incubate at 34 °C for 30 minutes, followed by T_1 relaxation time measurements at 34 °C.

HSA binding parameters were evaluated using the relaxation enhancement method[8], where the increment in the T_1 relaxation rate constants was attributed to the formation of a slowly moving adduct between the Fe_6L_4 cage and the HSA protein molecule. Furthermore, this increment is expressed by the enhancement factor (R^*_{1p}/ R_{1p}) which has contributions from paramagnetic (R_{1p}) and diamagnetic (R_{1d}) relaxation.

$$\frac{R^*_{1p}}{R_{1p}} = \frac{R^*_{1obs} - R^*_{1d}}{R_{1obs} - R_{1d}}$$

To evaluate the binding parameters, the following equilibrium is considered where K_a is the association/binding constant and n is the number of independent binding sites.

C + HSA ↔ C-HSA

$$K_a = \frac{[C-HSA]}{[C]_{free}\,[nHSA]_{free}} = \frac{[C-HS\ \ ]}{([C]_{tota}\ \ [C-HSA])\,([nHSA]_{total}\ \ [C-HSA])}$$ Equation S5

Also,

$$\frac{R^*_{1p}}{R_{1p}} = \frac{[C-HSA]}{[C]_{total}}(1.9) + \frac{([C]_{total-}\,[C-H\ \ ])}{[C]_{total}}$$ Equation S6

Combining equations S5 and S6, equation S7 is obtained which allows the non-linear fitting of the experimental data.

Equation S7,

$$\frac{R^*_{1p}}{R_{1p}} = (0.9)\frac{(K_a[C]_{total} + K_a[nHSA]_{total} + 1) - \sqrt{(K_a[C]_{total} + K_a[nHSA]_{total} + 1)^2 - 4K_a^2[C]_{total}[nHSA]_{total}}}{2K_a[C]_{total}} + 1.0$$

8.2. Fe_6L_4 Titration

HSA interaction with Fe_6L_4 was further explored by plotting the T_1 relaxation rates (R_{1obs}) observed with a fixed concentration of HSA (10 μM) against increasing concentrations of contrast agent (0-100 μM). Prepared solutions were allowed to incubate at 34 °C for 30 minutes, followed by T_1 relaxation time measurements on a Nanalysis 1.4 T benchtop NMR at 34 °C.

8.3. HSA competitive binding studies

The effect of well-established binders on HSA interactions with Fe_6L_4 cage was examined by evaluating the relaxivity in the presence of HSA (0.6 mM) with 0.6 mM of binders namely ibuprofen, warfarin, iodipamide, methyl orange and HPTS[9]. Solutions of 0.6 mM binder in 1x PBS were used as the blank solutions.

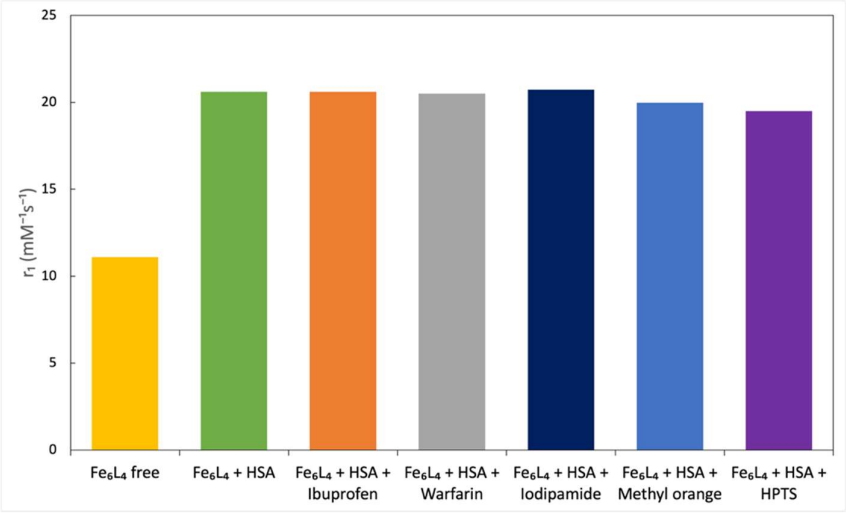

Figure S24. Relaxivity of Fe_6L_4 cage (80 μM) in 1x PBS, pH 7.4 in the presence of HSA (0.6 mM) with and without 0.6 mM of different binders. (HPTS refers to 8-hydroxypyrene-1,3,6-trisulfonic acid trisodium salt).

8.4. Poly-L-lysine study

T_1 relaxation time of the Fe_6L_4 cage (50 μM) in 1x PBS, pH 7.4 in the presence of 0.3 mM poly-L-lysine was measured. A solution of 0.3 mM poly-L-lysine in 1x PBS was used as the blank solution[9].

09. Mice MRI studies

All animal studies were carried out under a protocol approved by the Institutional Animal Care and Use Committee of the University at Buffalo. MR imaging was carried out on a 7T preclinical MRI (Bruker Biospin, Billerica MA) using ParaVision 360 and a 40 mm ID quadrature RF coil. BALB/c mice were anesthetized with isoflurane and respiration and temperature were monitored continuously with Model 1030 monitoring and gating system (SA Instruments, Stony Brook, NY). Following scout scans, baseline images were acquired in triplicate using a T_1 weighted, 3D segmented steady-state free precession (SSFP-FID) with the following parameters: TE/TR/FA = 2/6.5ms/10°, inter-segment repetition = 700ms, matrix = 128x96x96, field of view = 48x32x32mm. Compound was administered at a dose of 10 μmol cage /kg via tail vein and SPGR scans were acquired continuously up to 1 h after administration. Animals were re-imaged at 4 hours post-administration. Data sets were reconstructed with isotropic voxels and regions of interest for different tissues and vena cava were traced in Analyze 14 (AnalyzeDirect, Overland Park KS). MR signal was normalized using two sealed 1% agarose phantoms doped with 1mM and 2mM $CuSO_4$, respectively.

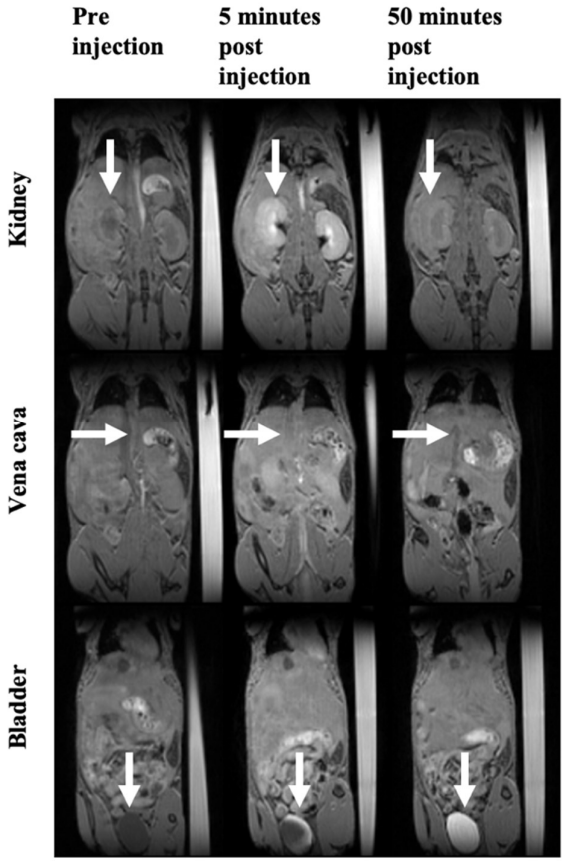

Figure S25. T_1-weighted MR images of kidney, vena cava and bladder after administration of 50 μmol/kg gadoterate meglumine.

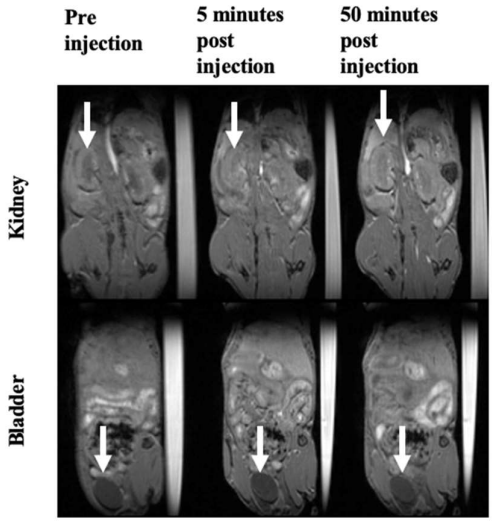

Figure S26. T_1-weighted MR images of kidney and bladder after administration of 10 µmol/kg cage Fe_6L_4.

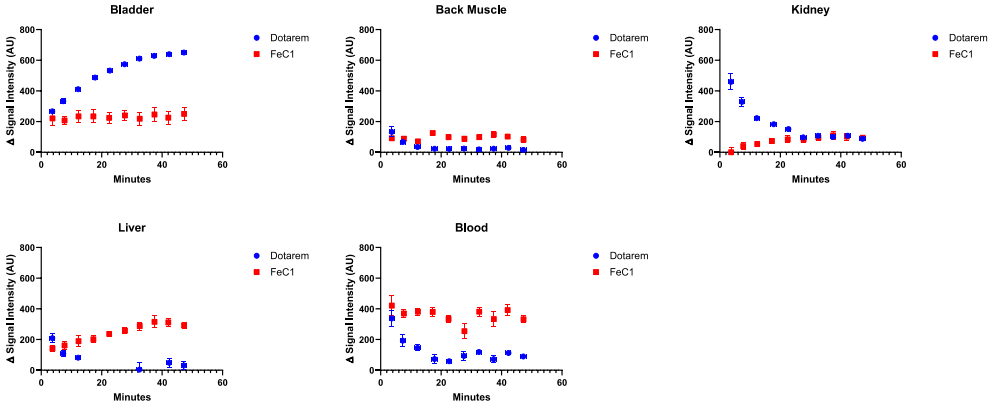

Figure S27. Data from T_1 weighted MRI of BALB/c mice showing signal enhancement at different time points.

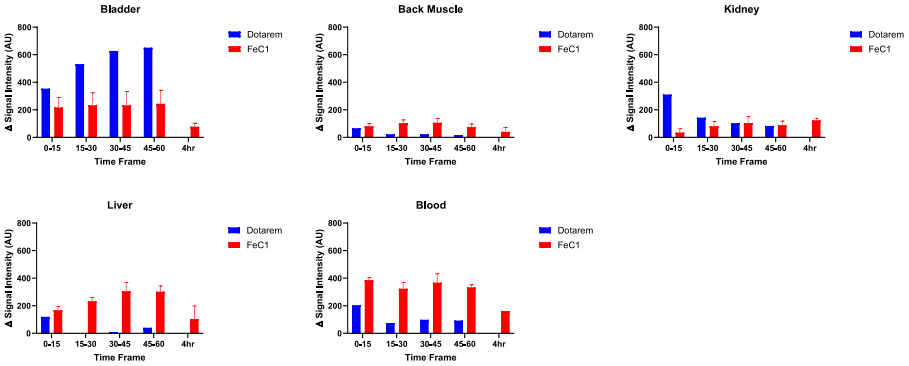

Figure S28. Data from T_1 weighted MRI of BALB/c mice showing pharmacokinetic clearance of Fe_6L_4 from different organs.

10. References

1. Feng, X., Chen, Y., Lei, Y., Zhou, Y., Gao, W., Liu, M., Huang, X. and Wu, H., Multifunctional properties of a star-shaped triphenylamine-benzene-1, 3, 5-tricarbohydrazide fluorescent molecule containing multiple flexible chains. *Chem Commun*, **2020**, *56*(88), 13638-13641.

2. He, C., Lin, Z., He, Z., Duan, C., Xu, C., Wang, Z. and Yan, C., Metal-Tunable Nanocages as Artificial Chemosensors. *Angew Chem Int Ed*, **2008**, *47*(5), 877-881.

3. Sokolow, G.E., Crawley, M.R., Morphet, D.R., Asik, D., Spernyak, J.A., McGray, A.R., Cook, T.R. and Morrow, J.R., Metal− Organic Polyhedron with Four Fe (III) Centers Producing Enhanced T1 Magnetic Resonance Imaging Contrast in Tumors. *Inorg Chem*, **2022**, *61*(5), 2603-2611.

4. Cineus, R., Abozeid, S.M., Sokolow, G.E., Spernyak, J.A. and Morrow, J.R., Fe (III) T_1 MRI Probes Containing Phenolate or Hydroxypyridine-Appended Triamine Chelates and a Coordination Site for Bound Water. *Inorg Chem*, **2023**, *62*(40), 16513-16522.

5. Evans, D. F., The determination of the paramagnetic susceptibility of substances in solution by nuclear magnetic resonance. *J Chem Soc* **1959**, 2003-5.

6. Bain, G.A. and Berry, J.F., Diamagnetic corrections and Pascal's constants. *J Chem Ed*, **2008**, *85*(4), 532.

7. Gale, E.M., Zhu, J. and Caravan, P., Direct measurement of the Mn (II) hydration state in metal complexes and metalloproteins through ^{17}O NMR line widths. *J Am Chem Soc*, **2013**, *135*(49), 18600-18608.

8. Aime, S., Botta, M., Fasano, M., Crich, S.G. and Terreno, E., Gd (III) complexes as contrast agents for magnetic resonance imaging: a proton relaxation enhancement study of the interaction with human serum albumin. *J Biol Inorg Chem*, **1996**, *1*, 312-319.

9. Stefania, R., Palagi, L., Di Gregorio, E., Ferrauto, G., Dinatale, V., Aime, S. and Gianolio, E., Seeking for Innovation with magnetic resonance imaging paramagnetic contrast agents: relaxation enhancement via weak and dynamic electrostatic interactions with positively charged groups on endogenous macromolecules. *J Am Chem Soc*, **2023**, *146*(1), 134-144.